Systems & Control Transactions

Research Article - Peer Reviewed Conference Proceeding
ESCAPE 35 - European Symposium on Computer Aided Process Engineering
Ghent, Belgium. 6-9 July 2025
Jan F.M. Van Impe, Grégoire Léonard, Satyajeet S. Bhonsale,
Monika E. Polańska, Filip Logist (Eds.)

PSE PRESS

Multiscale Modeling of Internal Reforming in Solid Oxide Fuel Cells: A Study of Electrode Morphology and Gradient Microstructures

Hamid Reza Abbasi[a], Masoud Babaei[a], and Constantinos Theodoropoulos[a,b]*

[a] Department of Chemical Engineering, The University of Manchester, Manchester, M13 9PL, UK
[b] Department of Chemical Engineering, National Technical University of Athens, Athens, 15772, Greece
* Corresponding Author: k.theodoropoulos@manchester.ac.uk.

ABSTRACT

This work presents a comprehensive multiscale model for Solid Oxide Fuel Cells (SOFCs), integrating microscale and macroscale simulations to analyze internal reforming and its impact on overall cell performance. The microscale model [1], [2] captures the intricate mass and charge transport phenomena at the pore scale of porous electrodes, resolving electrochemical reactions at the triple-phase boundaries and modeling chemical reactions at pore spaces. Simultaneously, the macroscale model provides a broader view of the entire cell's behavior by solving the same transport equations on a coarser computational mesh. The multiscale approach is particularly useful for addressing the challenges posed by simultaneous chemical and electrochemical reactions at the anode, which complicate the modeling of internal reforming. To overcome these challenges, a novel approach is introduced [3], spatially separating the regions of chemical and electrochemical activity in the pore scale domain by taking the electrochemical active layer thickness into consideration. The integrated multiscale model is applied to a complete internal reforming SOFC to explore how electrode morphology, particularly the use of gradient microstructures, influences cell performance.

Keywords: SOFC, Multiscale Model, Microscale Model, Internal Reforming, Gradient Microstructure

INTRODUCTION

Fuel cells are electrochemical devices that convert the chemical energy of a fuel directly into electricity, heat, and water through a reaction with oxygen, typically without combustion. They are highly efficient, scalable, and environmentally friendly, making them suitable for various applications, including power generation, transportation, and portable energy solutions. Among the different types of fuel cells, the choice depends on factors such as operating temperature, efficiency, and fuel flexibility.

Solid Oxide Fuel Cells (SOFCs) are a type of high-temperature fuel cell that operates at temperatures between 600°C and 1000°C. They use a solid ceramic electrolyte to conduct oxygen ions from the cathode to the anode, where they react with a fuel—such as hydrogen, natural gas, or biogas—to generate electricity. SOFCs are known for their high efficiency, fuel flexibility, and ability to use waste heat for additional power generation in combined heat and power (CHP) systems [4].

To use hydrocarbon fuels like methane (CH_4) in SOFCs, a reforming process, such as steam reforming, converts them into hydrogen-rich gas. SOFC high operating temperatures enable internal reforming, which simplifies system design and improves efficiency but requires careful management to prevent carbon deposition and ensure stable operation.

Internal reforming can be categorized into indirect and direct methods. Indirect reforming places the reformer outside the fuel cell but in thermal contact, using SOFC-generated heat to drive the reaction and minimizing carbon deposition risks [5]. Direct reforming occurs within the anode, where fuel and steam react together, streamlining the system and boosting efficiency but demanding precise control of temperature gradients to

prevent material degradation.

SOFCs exhibit defining features across various length scales, from the microscale structure of the porous electrodes to the macroscale design of the entire system. To predict their performance, different types of models have been developed, each focusing on a specific length scale. Microscale models focus on reactions and mass transport processes within the porous anode and cathode. At the macroscale, models address the transport phenomena within a single cell. By combining these models, researchers can better understand and enhance the performance of SOFCs across all relevant scales.

The microstructure design of the porous electrodes plays a critical role in defining the performance of SOFCs. Electrochemical reactions primarily occur at the triple-phase boundary (TPB), where the electrolyte, electrode, and gas phase meet. A high TPB density is essential for maximizing reaction sites and enhancing performance. Additionally, the tortuosity of the porous structure significantly affects gas and ion diffusion [6]. High tortuosity can hinder mass transport by increasing the effective path length for reactants and ions, leading to concentration gradients and performance losses. Optimizing the microstructure to balance TPB density and tortuosity is crucial for achieving efficient gas diffusion, ionic conductivity, and overall cell performance.

A multiscale model combines the strengths of these individual models to assess SOFC performance more comprehensively. By integrating physics across different length scales, such a model can capture detailed electrochemical and transport processes at the microscale while also considering cell-level features at the macroscale.

In the current study, a direct internal reforming SOFC is modelled using a multiscale framework. The model solves transport, chemical reactions, and electrochemical reactions at the microstructure level and transport equations, and chemical reactions at the cell level, syncing information between these two scales. Different microstructure configurations—conventional, lattice, and fibrous—are tested for both the anode and cathode to evaluate the benefits of each design.

METHODOLOGY

The methodology employs a multiscale framework that integrates two distinct models: a microscale model and a macroscale model. The microscale model focuses on the processes occurring within the porous microstructure of the electrodes. The macroscale model captures the transport behaviour at the cell level, addressing overall performance metrics. The computational domain is schematically shown in figure 1.

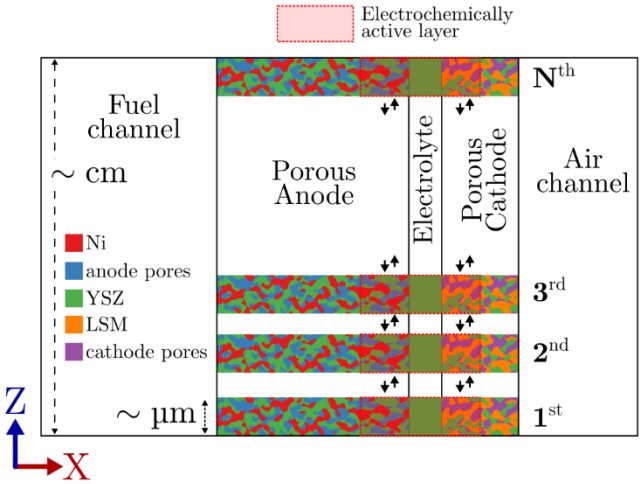

Figure 1. Schematic domain of the problem (microstructures and the entire cell)

Here only small "patches" of the microstructural domain are actually solved, as in the gap-tooth scheme [7,8] to reduce computational cost. The vertical arrows in fig 1 represent the fluxes between the microstructure patches.

To ensure consistency between the two scales, an iterative algorithm is employed. This algorithm minimizes discrepancies between the outputs of the microscale and macroscale models by iteratively adjusting parameters in the macroscale model. More specifically, the electrochemical reaction rates in the macroscale model are modified to better align with the detailed microscale predictions since there is a more fundamental definition for the kinetics of electrochemical reactions at the microscale. To describe the rate of electrochemical reactions at microscale we have used a lineal exchange current density, which is per length of TPB. Whereas for the macroscale model the kinetics of electrochemical reactions could only be described based on area or volume. Since electrochemical reactions are essentially heterogeneous and take place on the TPB lines in space (as opposed to a homogeneous reaction that take place in space) a lineal exchange current density is fundamentally more accurate than an area-averaged or volume-averaged definition.

By iterating between the models, the framework converges to a solution that harmonizes the behaviour across scales. This idea is explained in more detail in our recent work [2].

The convective and diffusive mass transport is dictated by the following equation:

$$\overbrace{\nabla \cdot \left(D_i^{\text{eff}} \nabla C_i\right)}^{\text{diffusive}} - \overbrace{\nabla \cdot (\vec{V} C_i)}^{\text{convective}} + S_i = 0 \qquad (1)$$

Here, D_i^{eff} is the effective diffusivity of component i into the gaseous mixture, C_i is mass density of i_{th} gaseous component, V is fluid velocity. The term S_i is the non-

linear source term that exists due to chemical and electrochemical reactions that consume or produce a particular component in the mixture. In the microscale model the convective term is disregarded due to the small pore sizes in the porous electrodes.
The ion conduction is modeled using this equation:

$$\nabla \cdot \left(\sigma_{\text{ion}}^{\text{eff}} \nabla \phi_{\text{ion}}\right) + S_{\text{ion}} = 0 \quad (2)$$

Here, $\sigma_{\text{ion}}^{\text{eff}}$ is the effective diffusivity of ions in the ion conductive material and S_{ion} is the non-linear source term due to electrochemical reactions.

The two main chemical reactions considered for internal reforming are Steam-Methane Reforming (SMR) and the Water-Gas Shift (WGS) reaction. In SMR, methane reacts with steam to produce hydrogen and carbon monoxide: $CH_4 + H_2O \rightarrow CO + 3H_2$. The WGS reaction further converts carbon monoxide and steam into additional hydrogen and carbon dioxide: $CO + H_2O \rightarrow CO_2 + H_2$. These reactions are crucial for generating the hydrogen necessary for electrochemical reactions at the anode. The following equations describe the rate of SMR and WGS [9]:

$$r_{\text{SMR}} = k_{\text{SMR}} p_{\text{CH4}} \, exp\left(-\frac{E_{\text{SMR}}^{A}}{RT}\right) \quad (3)$$

$$r_{\text{WGS}} = k_{\text{WGS}} p_{\text{CO}} \left(1 - \frac{p_{\text{CO2}} p_{\text{H2}} / p_{\text{CO}} p_{\text{H2O}}}{K_{eq}}\right) \quad (4)$$

Here, E_{SMR}^{A} is the SMR reaction activation energy, k_{SMR} is pre-exponential factor of SMR. For WGS, k_{WGS} is the reaction rate constant, and K_{eq} is the equilibrium constant.

Modelling internal reforming presents a significant challenge when it comes to simultaneously simulating chemical and electrochemical reactions. These two processes occur in tandem, but their interplay complicates the formulation of the problem. One specific issue is the modelling of concentration overpotential, which is traditionally defined in terms of the bulk pressure of hydrogen. In the case of internal reforming SOFCs, if the hydrogen pressure at the inlet is zero, the concentration overpotential would theoretically become infinite, which is physically unrealistic and resulting in zero-division error. This presents a fundamental problem because it suggests an unbounded overpotential. To address this, we propose a solution that involves artificially separating the regions where electrochemical and chemical reactions occur.

In our model, the anode side of the microstructure is divided into two distinct zones: the region closer to the electrolyte, where electrochemical reactions dominate, is treated as an electrochemical-only zone, while the region farther away from the electrolyte, where chemical reactions dominate, is treated as a chemical-only zone. This separation allows us to avoid the unphysical infinite concentration overpotential by ensuring that each region is simulated with the appropriate reaction mechanism. This is schematically shown in Figure 2.

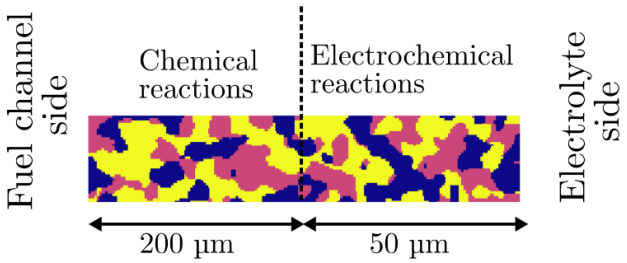

Figure 2. Separation of anode side into two regions

Electrochemical reactions are dominant in a very thin layer close to the electrolyte called the "electrochemical active layer". The length of this layer is reported to be smaller than $50\ \mu m$ [10]. The concept is that the rate of electrochemical reactions is negligible on the left side of Figure 2, while the rate of chemical reactions is negligible on the right side. Therefore, it is assumed that these negligible rates are effectively zero.

Different microstructure designs tested in this study are shown in Figure 3. The reasoning behind why each design is selected is further explained in our recent manuscript [11].

RESULTS AND DISCUSSION

Model Validation

The model is firstly validated against experimental measurements of Rogers et al.12]. The polarization curve is selected for the basis of the comparison, and it is shown in Figure 4. In this figure the experimental data points are shown with black dots, and results of the macroscale and multiscale models are shown with red and green lines, respectively. The red area shows the region where the polarization curve varies with a ±10% change in the calibration parameter of macroscale model.

From figure 4, it is obvious that both the calibrated macroscale model, and multiscale model, are capable of explaining the polarization curve of the cell. However, the two models differ in terms of calibration requirements. The macroscale model requires calibration using experimental data, with the calibration parameter being the area-averaged exchange current density, which accounts for the overall electrochemical activity in the cell. In contrast, the multiscale model does not require such calibration. This is because it uses a more fundamental definition of exchange current density, namely the lineal exchange current density. As a result, the multiscale model offers a more fundamental approach without the need for calibration, while the macroscale model relies on fitting to ample experimental data to accurately represent the system's behaviour.

It is also important to note that the point of using a multiscale model is not to achieve a better match with experimental results for a given set of datapoints on the polarization curve. Rather, the goal here is to explore

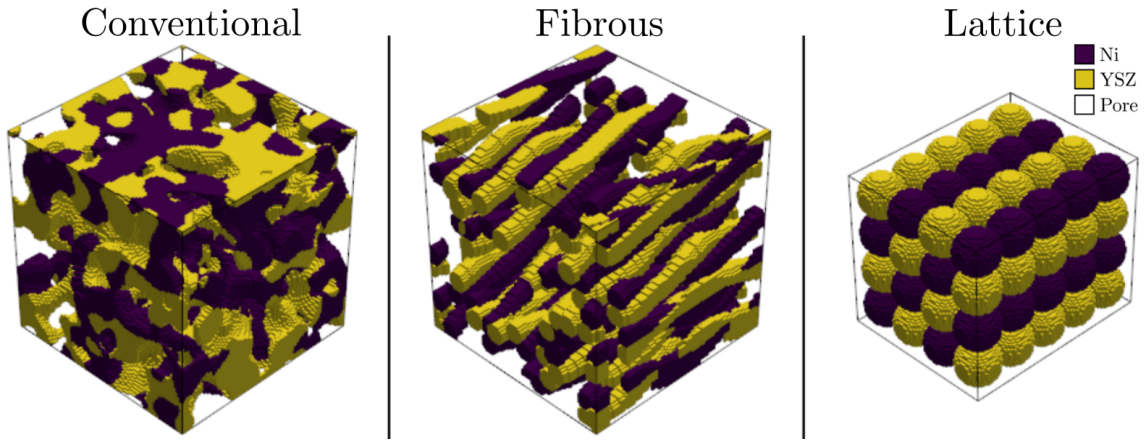

Figure 3. Different microstructure designs

different designs with varying microscopic and macroscopic features, especially for which no measured experimental data is available. This allows for the investigation of new designs and configurations that are not constrained by the existing experimental dataset.

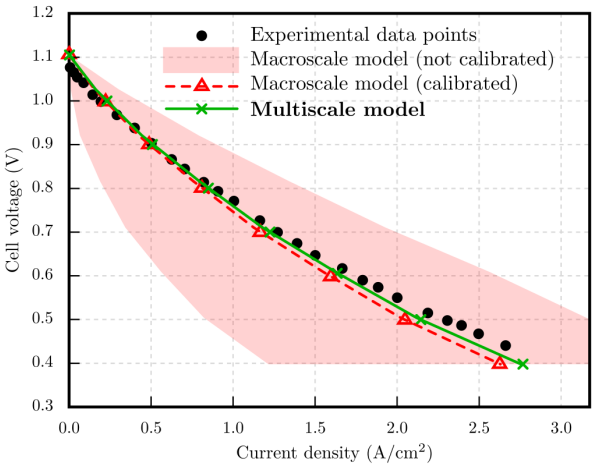

Figure 4. Polarization curve of different models compared with experimental measurements [9]

Spatial Distribution of Field Variables Across the Anode

Variation of concentration of different components across the anode is shown in figure 5. This figure is for the case of conventional microstructure (refer to figure 2). Five different components exist in the gaseous mixture in the anode side.

At the anode inlet, only CH_4 and H_2O have non-zero concentrations. Due to SMR, the concentration of CH_4 decreases monotonically toward the electrolyte side. Based on the chemical reactions, the concentration of H_2O would be expected to decrease monotonically because it is consumed in both SMR and WGS. However, due to the production of H_2O in the electrochemically active layer, its concentration levels off as it approaches this layer and then begins to increase. A similar explanation, but with the opposite reasoning, applies to the hydrogen concentration. Due to SMR and WGS, its concentration increases as it approaches the electrochemically active layer, only to level off and then decrease upon entering this layer.

To validate the assumption of a negligible chemical reaction rate near the electrolyte and a negligible electrochemical reaction rate in the remaining of the porous anode, these rates are compared in Figure 6, which is based on the case of a conventional microstructure. It can be observed that the rate of electrochemical reactions levels off after the first $50\ \mu m$ near the electrolyte. This occurs because the electrochemical activity becomes limited by the availability of reactants in this region. Similarly, the rate of the SMR reaction drops significantly as it approaches this region, which can be attributed to the limited availability of CH_4 approaching the electrochemically active layer.

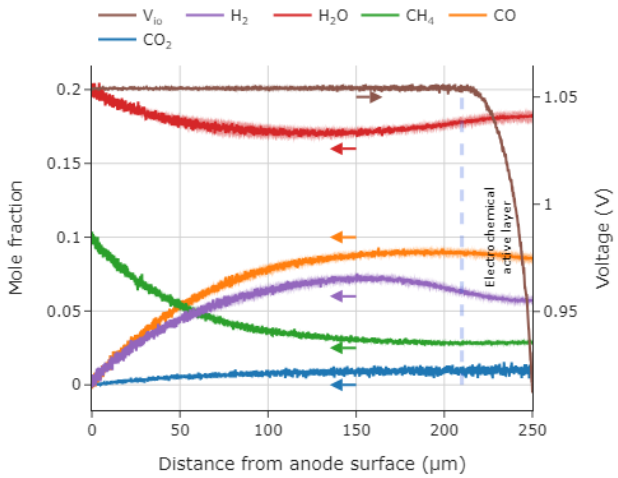

Figure 5. Concentration of different species across the anode

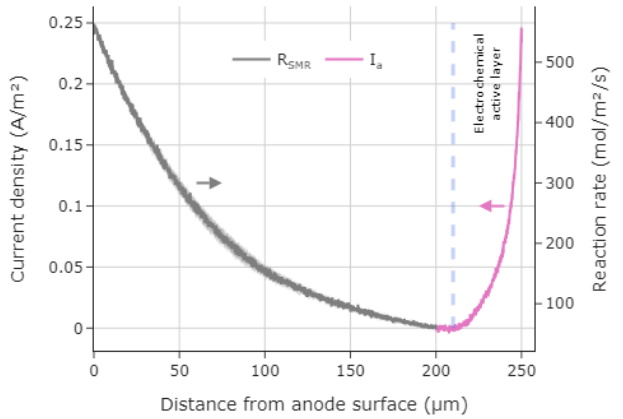

Figure 6. Comparison of electrochemical and chemical reactions rates

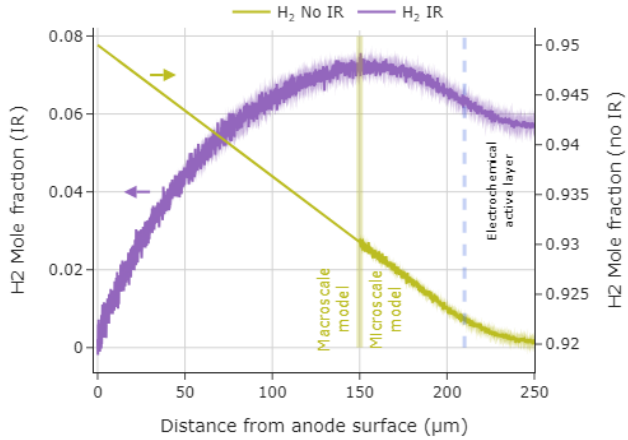

Figure 7. Evolution of hydrogen mole fraction across the width of the anode surface for the case of no IR and IR.

Different Morphologies and Gradient Microstructures

Gradient microstructures are designed so that the volume fraction of the ion-conducting phase (YSZ, in this case) linearly decreases as we move further from the electrolyte. If the volume fraction of the ion-conducting phase behaves in the opposite manner, the resulting microstructure does not offer any benefits. This phenomenon is discussed in more detail in our recent manuscript [11]. Gradient microstructures have been synthetically generated using the framework discussed in our previous work [11] with f_G being defined as $f_G = \frac{\overline{v_f^{YSZ}} - v_f^{YSZ}(x = x_{electrolyte})}{\overline{v_f^{YSZ}}}$.

The results in figure 8 shows the TPB density and current density of IR cell performing under $V = 0.4\ [V]$. The figure indicates that a microstructure with a stronger gradient of volume fraction leads to a greater reduction in TPB density. This occurs because, at both ends of a gradient microstructure, the volume fractions of the three phases deviate significantly from each other. Such imbalance makes the microstructure less optimal for TPB formation, as TPB density in conventional designs is maximized when the volume fractions of the three phases are nearly equal. While TPB density decreases as the gradient strength increases, the current density (a measure of the cell's overall performance) initially rises (in the G^+ region) before eventually declining (in the G^- region). The decrease in current density in the G^- region corresponds to the drop in TPB density. However, the initial rise in current density in the G^+ region, despite the reduction in TPB density, can be explained by improved ion conduction. This enhanced ion conduction promotes higher rates of electrochemical reactions at the remaining TPB sites, leading to better overall performance initially.

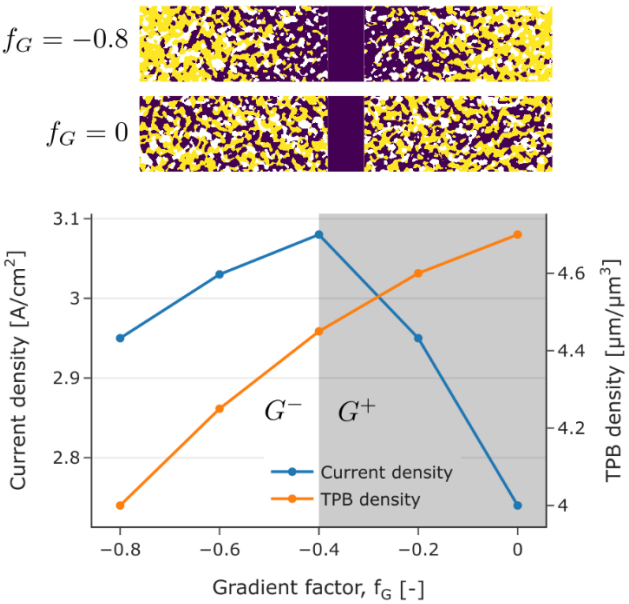

Figure 8. Performance of gradient microstructures

Different designs are tested for the microstructure of porous anode and cathode. Each design is tested for both sides of the cell—anode and cathode. In other words, the microstructural designs of the anode and cathode are assumed to be identical. To compare the performance of different designs, current density was measured at an operating voltage of 0.4 volts. Results indicate that the fibrous design increased current density by approximately 48%, from 2.74 A/cm² (conventional design) to 4.05 A/cm². In contrast, lattice structures significantly enhanced performance, increasing current density by roughly 4.4 times, from 2.74 A/cm² to 12.05 A/cm². It is important to acknowledge that the lattice structures depicted in Figure 3 represent a highly optimized theoretical design. Current state-of-the-art fabrication techniques cannot achieve the precise, highly ordered placement of nanoparticles required to realize these structures.

CONCLUSIONS

This study employed a multiscale model to predict the performance of direct internal reforming solid oxide fuel cells, eliminating the need for calibration typically required with macroscale models. The model was used to evaluate various microstructure designs, including gradient microstructures, to assess their potential benefits. Results demonstrate the successful application of the multiscale model in predicting the polarization curve of a complete cell. Furthermore, the study revealed that certain gradient microstructures can outperform the counterpart non-gradient designs.

ACKNOWLEDGEMENTS

The project is implemented within the framework of the National Recovery and Resilience Plan "Greece 2.0" and has been financed by the European Union (NextGeneration EU)

REFERENCES

1. Abbasi, H. R., Babaei, M., Rabbani, A., & Theodoropoulos, C. Multi-scale model of solid oxide fuel cell: enabling microscopic solvers to predict physical features over a macroscopic domain. In *Computer Aided Chemical Engineering* (Vol. 52, pp. 1039-1045). Elsevier. (2023)
2. Abbasi, H. R., Babaei, M., & Theodoropoulos, C. Multiscale Modeling of Solid Oxide Fuel Cells Using Various Microscale Domains Across the Length of the Cell. In *Computer Aided Chemical Engineering* (Vol. 53, pp. 2317-2322). Elsevier.H. (2024)
3. Abbasi, H., Babaei, M., & Theodoropoulos, C. Multiscale Simulation of Internal Reforming Solid Oxide Fuel Cells to Capture Complex Reaction Phenomena. In *Electrochemical Society Meeting Abstracts prime2024* (No. 48, pp. 3310-3310). The Electrochemical Society, Inc. (2024, November)
4. Singh, M., Zappa, D., & Comini, E. Solid oxide fuel cell: Decade of progress, future perspectives and challenges. *International Journal of Hydrogen Energy*, *46*(54), 27643-27674. (2021)
5. Fan, L., Li, C. E., Aravind, P. V., Cai, W., Han, M., & Brandon, N. Methane reforming in solid oxide fuel cells: Challenges and strategies. *Journal of Power Sources*, *538*, 231573. (2022)
6. Tseronis K, Bonis I, Kookos IK, Theodoropoulos C, Parametric and transient analysis of non-isothermal, planar solid oxide fuel cells. *International journal of hydrogen energy* 37 (1), 530-547 (2012)
7. Kevrekidis I.G., Gear W.C., Hyman J,M., Kevrekidis P.G, Runborg O. & Theodoropoulos C. Equation-free, coarse-grained multiscale computation: Enabling mocroscopic simulators to perform system-level analysis. Commun. Math. Sci. 1(4) 715-762 (2003).
8. Armaou A., Kevrekidis IG, Theodoropoulos C. Equation-free gaptooth-based controller design for distributed complex/multiscale processes. Comput. Chem. Eng. 29(4), 731-740 (2005).
9. Tseronis, K., Fragkopoulos, I. S., Bonis, I., & Theodoropoulos, C. Detailed Multi-dimensional Modeling of Direct Internal Reforming Solid Oxide Fuel Cells. *Fuel Cells*, *16*(3), 294-312. (2016)
10. Kishimoto, M., Iwai, H., Saito, M., & Yoshida, H. Quantitative evaluation of solid oxide fuel cell porous anode microstructure based on focused ion beam and scanning electron microscope technique and prediction of anode overpotentials. *Journal of Power Sources*, *196*(10), 4555-4563. (2011)
11. Abbasi, H., Rabbani, A., Babaei, M., & Theodoropoulos, C. A pore-scale computational framework for enhancing solid oxide fuel cell performance through the design of anode porous configurations. *Journal of The Electrochemical Society. In press* https://doi.org/10.1149/1945-7111/adbfc4 (2025).
12. Rogers, W. A., Gemmen, R. S., Johnson, C., Prinkey, M., & Shahnam, M. Validation and application of a CFD-based model for solid oxide fuel cells and stacks. In *International Conference on Fuel Cell Science, Engineering and Technology* (Vol. 36681, pp. 517-520). (2003, January)